

# We are IntechOpen, the world's leading publisher of Open Access books Built by scientists, for scientists

6,900

Open access books available

186,000

International authors and editors

200M

Downloads

Our authors are among the

154

Countries delivered to

TOP 1%

most cited scientists

12.2%

Contributors from top 500 universities



WEB OF SCIENCE™

Selection of our books indexed in the Book Citation Index  
in Web of Science™ Core Collection (BKCI)

Interested in publishing with us?  
Contact [book.department@intechopen.com](mailto:book.department@intechopen.com)

Numbers displayed above are based on latest data collected.  
For more information visit [www.intechopen.com](http://www.intechopen.com)



# Acoustical Measurement and Fan Fault Diagnosis System Based on LabVIEW

Cao, Guangzhong  
Shenzhen University,  
P.R.China

## 1. Introduction

It is difficult to diagnose the reasons of fan fault because of lacking mapping relationship between fault and symptom. Current fault diagnosis methods for rotating machinery such as vibration detection, temperature detection and so on, have to use contact measurement. However, those methods cannot be available for many important field devices.

Either in time domain or in frequency domain the local characteristics of wavelet are good in extracting time-varying signal characteristics. Neural network has a strong capability to identify the multi-dimensional and non-linear model. Therefore, it is possible to improve the accuracy of diagnosis system by combination of wavelet and neural network. In this chapter, an intelligent fan fault diagnosis system is presented where the noise produced by fan is considered the diagnosis signal, a non-contact measurement is adopted and the non-linear mapping from feature space to defective space using the wavelet neural network is performed.

## 2. Basic concept and theory

### 2.1 Acoustical measurement basis

#### 2.1.1 Basic acoustical parameters

Analysis of sound and acoustics plays a role in such engineering tasks as product design, production test, machine performance, and process control. In order to perform analysis of sound and acoustics, we should know the parameters and process for acoustical measurement. In general, there are many physical parameters that should be measured in acoustical measurement such as sound pressure, sound intensity, sound power and others. The most common acoustical measurement parameters are as follows:

##### 1. Sound pressure (acoustic pressure) $P$

Sound pressure is the local pressure deviation from the ambient atmospheric pressure caused by a sound wave. The value of the rapid variation in air pressure due to a sound wave, measured in pascals. *Instantaneous* sound pressure is the peak value of air pressure and its value reflects the intensity of sound. Usually, *sound pressure* is the effective sound pressure for short. *Effective sound pressure* is the RMS value of the instantaneous sound pressure taken at a point over a period of time as:

$$P = \sqrt{\frac{1}{T} \int_0^T P^2(t) dt} \quad (2-1)$$

where  $P(t)$  is instantaneous sound pressure,  $T$  is the time interval averaging.

## 2. Sound pressure level $L_p$

Sound pressure level  $L_p$  is a logarithmic measure of the effective sound pressure of a sound relative to a reference value. It is measured in decibels (dB). For sound in air, it is customary to use the value  $2 \times 10^{-5} \text{ pa}$ . The formula for calculating the sound pressure level is defined as (Cao & Ruan, 2002; Donald & Hall, 1987) :

$$L_p = 10 \lg \frac{P^2}{P_0^2} = 20 \lg \frac{P}{P_0} \quad (2-2)$$

where  $L_p$  is sound pressure level (dB),  $P_0$  is the reference sound pressure ( $2 \times 10^{-5} \text{ pa}$ ),  $P$  is effective sound pressure.

## 3. Sound level $L$ and A-weighted sound level $L_A$

Sound pressure level only reflects the sound intensity of human feeling of loudness, but the human ear's sensitivity is strongly dependent on frequency. Loudness level and loudness of the sound that reflect people's subjective feelings are too complex, so the concept of sound level, i.e. the concept of the weighted sound pressure level is proposed. Sound level is the sound pressure level obtained by weighting with some weighted networks. To simulate the human ear's sensory characteristics of loudness, the weighting network classifications are divided into A, B and C-weighted networks. The simplest and probably most widely used measure of noise is the A-weighted sound level, expressed in dBA. A-weighting assigns to each frequency a "weight" that is related to sensitivity of the ear at that frequency (Kinsler et al., 2000).

## 4. Equivalent continuous sound level $L_{eq}$

For rolling or discontinuous noise, the equivalent continuous sound level is needed to evaluate the impact of noise on people. Equivalent continuous A-weighted sound pressure level is widely used as an index around the world. It is defined as "the A-weighted sound pressure level of a noise fluctuating over a period of time  $T$ , expressed as the amount of average energy." It is expressed as:

$$L_{eq} = 10 \lg \left( \frac{\Delta t}{T} \sum_{i=1}^n 10^{0.1 L_{Ai}} \right) = 10 \lg \left( \frac{1}{n} \sum_{i=1}^n 10^{0.1 L_{Ai}} \right) = 10 \lg \left( \sum_{i=1}^n 10^{0.1 L_{Ai}} \right) - 10 \lg(n) \quad (2-3)$$

where  $T$  denotes the length of sampling,  $\Delta t$  is the sampling interval,  $n$  is the sampling number,  $L_{Ai}$  is instantaneous A-weighted sound level,  $L_{eq}$  is equivalent continuous sound level.

## 5. Statistical sound level $L_N$

Because environmental noise often fluctuates over a wide range of time and space, no single value describes the noise accurately. Another useful set of parameters is needed, which are statistical sound levels by using probability or cumulative probability to indicate the appearance of different sound level. Statistical sound level  $L_N$  indicates that the probability of appearance of the sound level greater than this sound level is  $N\%$ . The most common levels used are  $L_{10}$ ,  $L_{50}$  and  $L_{90}$ .  $L_{10}$  is equivalent to the average noise level of peak,  $L_{50}$  is equivalent to median noise level, and  $L_{90}$  is equivalent to background noise.

### 2.1.2 Sound level meter

Sound level is a fundamental physical quantity of acoustical measurement. Sound level meter (SLM) is a basic instrument for measuring noise and sound levels in a specified manner. There are many categories of sound level meters due to different classification criteria. In terms of different uses, sound level meter can be classified into ordinary sound level meter, pulse sound level meter, integrating sound level meter, statistical-integral sound level meter and others. In terms of accuracy level, SLM can be divided into type 0 SLM (as in a laboratory, a standard SLM with an accuracy of  $\pm 0.4$  dB), type-I SLM (a precision SLM with an accuracy of  $\pm 0.7$  dB), type-II SLM (a general purpose SLM with an accuracy of  $\pm 1.0$  dB), type-III SLM (a universal SLM with accuracy of  $\pm 2.0$  dB); According to different size of volume, a SLM can be divided into desktop SLM, portable SLM, pocket-size SLM and so on.

Although there are many types of SLM, the working principle of all categories of SLM is identical in nature. The difference is some additionally special features which enable SLM to carry out various measurements such as adding integral circuit can help to measure the equivalent continuous sound level. In acoustics, a SLM usually consists of a microphone, amplifiers, an attenuator, frequency weighted networks, detector, indicator and power supply, etc (Cao & Ruan, 2002; Cao et al. 2004; Donald & Hall, 1987; Kinsler et al., 2000; Ruan & Cao, 2006). The working principle of the SLM is shown in Fig.2.1.

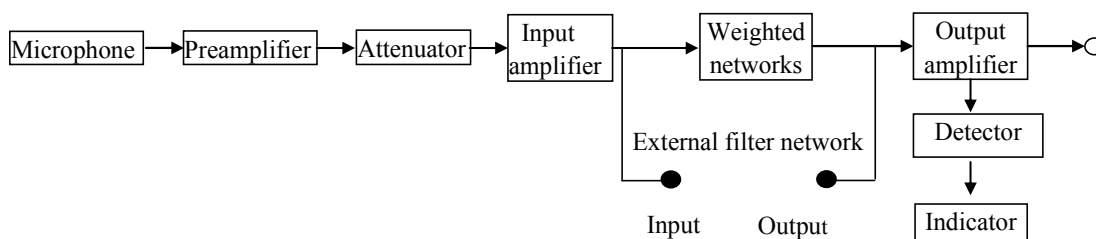


Fig. 2.1. SLM composition

In this figure, the microphone is the most critical element for acoustical measurement which is an acoustic-to-electric transducer or sensor that converts sound pressure signal into an electrical signal. In terms of different principles for conversion of mechanical signals into electrical signals, the types of microphone are divided into three main categories: dynamic microphone, piezoelectric microphone and condenser or capacitor microphone. The microphone applied in SLM requires a wide frequency and high dynamic range, low distortion, high sensitivity, small temperature coefficient and so on. Dynamic microphone has larger volume with uneven frequency response. Therefore it is vulnerable to electromagnetic interference. Piezoelectric microphone is susceptible to temperature changes with poor stability. Thus, the use of the above microphones in SLM is limited. The condenser microphone overcomes the above shortcomings and is usually employed in acoustic measurement field. However, it has the disadvantage of high internal resistance which requires an impedance converter, amplifier and attenuator with some designated voltage supplier.

Preamplifier is needed to meet the requirements of using capacitor microphone because the capacitor microphone has high internal resistance, low capacitance (usually only tens of picofarad (pF), and even several pFs). If a capacitor microphone is connected to an amplifier

whose input capacitance is similar to the capacitor microphone, it may reduce the sensitivity of the microphone. If the amplifier input resistance is too low, then the low frequency sensitivity of the capacitor microphone will be reduced, that is, the frequency range of the capacitor microphone is limited. Therefore, suitable preamplifier is needed for the SLM with a capacitor microphone.

**Amplifier:** Capacitor microphone converts sound into electrical signal. The signal is generally very weak, not enough to drive display in an indicator, thus, amplifier circuit is needed to amplify the electrical signal to drive detector circuit and indicating instrument. The amplifier of a SLM requires a certain amplifier factor, a certain dynamic range, a wide frequency range and small level of non-linear distortion.

**Attenuator:** The SLM measures not only the weak signal but also the strong one. It should have the large dynamic measurement range. However the detector and the indicator of a SLM may not have wide measurement range, so we should use the attenuator to attenuate the input signal, acquire the appropriate command from the indicator, and enlarge measurement range.

**Weighted network:** Weighted network of a SLM is a set of electric networks which undertake frequency filtering according to certain weighted characteristics, usually formed by a multi-stage RC network. Because 'A' sound level is widely used, almost all SLMs have A-weighted network. Although some of SLMs also have B-weighted network and C-weighted network. Even some of SLMs also have "linear" frequency response, which is used to measure the non-weighted sound pressure levels.

**Detector and indicator:** Detection circuits used to change the output signal of the amplifier into a DC signal to gain proper instructions in the indicating instrument. Usually the size of the signal is measured by the peak, average and RMS. In the measurement of sound level, the most commonly used is the RMS.

## **2.2 Wavelet theory and Mallat algorithm**

### **2.2.1 Wavelet theory**

A wavelet is a "small wave", which has its energy concentrated in time to give a tool for the analysis of transient, non-stationary, or time-varying phenomena (Burrus, 2005). It still has the oscillating wave-like characteristic and the ability to allow simultaneous time and frequency analysis.

As a new mathematical branch, wavelet theory has made an important breakthrough and development in a lot of research fields such as signal processing, image processing, pattern recognition, and so on.

The concept of wavelet transform was first introduced by a France geologist J. Morlet when he analyzed geological data in 1970s. He applied it successfully in seismic signal analysis. Later a famous France mathematician Y.Meyer carried out a series of theoretical researches on wavelet. In 1986, based on the multi-resolution analysis, S.Mallat proposed the dyadic wavelet transform and its fast algorithm—Mallat algorithm, which established the foundation for wide area applications of wavelet analysis. Wavelet analysis is a kind of mathematical method that can carry out partial analysis of signal in time and frequency domain at the same time. Its sampling step length in time domain for signal with different frequency is diverse from each other, that is, there is higher frequency resolution and lower time resolution for lower frequency signal, and vice versa. That is why wavelet analysis has adaptability to signal and wavelet transform is regarded as mathematical microscope.

### 2.2.2 Wavelet transform

Wavelets consist of a family of mathematical functions used to represent a signal both in time and frequency domain. A wavelet transform (WT) decomposes a temporal signal into a set of time-domain basis functions with various frequency resolutions. The WT is computationally similar to the windowed short-term Fourier Transform (WFT). However, unlike the sine and cosine functions used in the WFT, the wavelet functions used in the WT are localized in spaces. Thus, the wavelet transform can decompose a signal into two sub-signals: *approximations* and *details* (Adeli & Jiang, 2009). The *approximations* represent the high-scale, low-frequency components of the signal, while the *details* represent the low-scale, high-frequency components. Therefore, compared with the Fourier transform, the wavelet transform provides a more effective representation of discontinuities in signals and transient functions.

If the time series with  $N$  measured data points,  $f(t)$ , is considered to be a square integrable function (i.e., the integral of its square is finite), both continuous wavelet transform (CWT) and discrete wavelet transform (DWT) can be used to analyze the time series data. The CWT of  $f(t)$  is defined as (Mallat, 1989):

$$W_f(a,b) = \int_{-\infty}^{\infty} f(t)\psi_{a,b} dt \quad (2-4)$$

The two-dimensional wavelet expansion functions  $\psi_{a,b}$  are obtained from the basic function (also known as mother or generating wavelet)  $\psi(t)$  by simple scaling and translation:

$$\psi_{a,b}(t) = \frac{1}{\sqrt{|a|}} \psi\left(\frac{t-b}{a}\right), a, b \in R, \psi \in L^2(R) \quad (2-5)$$

where  $\in$  denotes membership,  $t$  is the time variable, the parameters  $a$  ( $\neq 0$ ) and  $b$  denote the frequency (or scale) and the time (or space) location, respectively, and  $R$  is the set of real numbers. The notation  $L^2(R)$  represents the square summable time series space of the data, where the superscript 2 denotes the square of the modulus of the function.

To avoid intensive computations for every possible scale  $a$  and dilation  $b$ , the dyadic values are often used for both scaling and dilation in discrete wavelet transform as follows:

$$a_j = 2^j, b_{j,k} = k2^j, j, k \in Z \quad (2-6)$$

where  $k$  and  $j$  denote the time and frequency indices, respectively, and  $Z$  is the set of all integers.

Substituting Equation (2-6) into Equation (2-5), the following wavelet expansion function is obtained:

$$\psi_{j,k}(t) = 2^{-j/2} \psi(2^{-j}t - k), j, k \in Z, \psi \in L^2(R) \quad (2-7)$$

So Equation (2-4) is rewritten as:

$$W_f(j,k) = 2^{-j/2} \int_{-\infty}^{\infty} f(t)\psi(2^{-j}t - k) dt, j, k \in Z, \psi \in L^2(R) \quad (2-8)$$

which is the DWT of the time series  $f(t)$ .

The DWT represented by Equation (2-8) aims to preserve the dominant features of the CWT from Equation (2-4) in a succinct manner. Conceptually, the DWT can be considered as a judicious sub-sampling of CWT coefficients with just dyadic scales (i.e.,  $2^{j-1}$ ,  $j = 1, 2, \dots, L$ , where  $L$  is the maximum number of the decomposition level). Compared with the DWT, the CWT can represent the physical system more accurately as it makes very subtle information visible, but it requires more intensive computations for integrating over every possible scale,  $a$ , and dilation,  $b$ .

The time series can be reconstructed by inverse of the CWT of Equation (2-4) in the double-integral form or the DWT of Equation (2-5) in the double-summation form. In terms of DWT, the time series  $f(t)$  is reconstructed by:

$$f(t) = \sum_j \sum_k a_{j,k} \psi_{j,k}(t) \quad (2-9)$$

where the coefficients of the series  $\{a_{j,k}\}$  are calculated as follows:

$$a_{j,k} = \langle f(t), \psi_{j,k}(t) \rangle \quad (2-10)$$

in which  $\langle f(t), \psi_{j,k}(t) \rangle$  represents the inner product of two functions  $f(t)$  and  $\psi_{j,k}(t)$ .

### 2.2.3 Mallat algorithm

The role of the fast algorithm of wavelet transform Mallat is the same as Fast Fourier Transform in Fourier transform. It decomposes signals orthogonally and effectively into different independent wave bands. The nature of Mallat algorithm is that there is no need to know the specific structure of scaling function and wavelet function and signal decomposition and reconstruction can be achieved by the coefficients of Mallat algorithm. Furthermore the length of the coefficients can be reduced in half for each decomposition, thus the calculated amount of wavelet transform is significantly decreased. Thus the application and development of wavelet is greatly pushed forward (Mallat,1992).

Suppose the discrete sample sequence of the signal  $f(t)$  is expressed by  $f(n)$ ,  $n = 1, 2, \dots, N$ , if  $f(n)$  is the approximation of signal at scale  $j = 0$ , it is marked by  $c_0(n) = f(n)$ . Therefore, the decomposing formula can be described by:

$$c_{j+1}(n) = \sum_{m \in \mathbb{Z}} c_j(m) h(m - 2n) \quad (2-11)$$

$$d_{j+1}(n) = \sum_{m \in \mathbb{Z}} c_j(m) g(m - 2n) \quad (2-12)$$

The reconstruction formula can be represented by:

$$c_j(n) = \sum_{m \in \mathbb{Z}} (c_{j+1}(m) h(n - 2m) + d_{j+1}(m) g(n - 2m)) \quad (2-13)$$

In Equation (2-11)-(2-13),  $m = 0, 1, 2, \dots, N - 1$ , and  $N$  is the length of the input sequence,  $c_j$  is the approximate coefficient at  $j$ th layer;  $d_j$  is the detail coefficient at  $j$ th layer,  $h$  is the low-pass filter coefficients of the used wavelet;  $g$  is the high-pass filter coefficients of the applied wavelet.

## 2.3 BP neural network

### 2.3.1 Artificial neural networks

An Artificial Neural Networks (ANN) is a nonlinear large-scale adaptive system based on numerous processing units. It is proposed and developed from the results of scientific research in the modern neuro-physiology to simulate the simple model of human neural cell with capability of generalization and learning. It is essentially a simple mathematical model representing a nonlinear mapping function from a set of input  $X$  to output  $Y$ , i.e.,  $f: X \rightarrow Y$ . The most commonly used ANN model is the feedforward neural network (Adeli, 2009 & Rumelhart et al., 1986). This network usually consists of input, hidden, and output layers. The information moves only in the forward direction, from the input nodes, through the hidden nodes to output nodes. There are no loops in the network.

For example, Fig. 2.2 shows a widely used three-layer feedforward ANN model, with arrows depicting the dependencies between variables at each layer. Its single output  $\hat{y}$  (i.e., model prediction) is the nonlinear weighted sum of the inputs  $X$ . In Fig. 2.2, the input vector  $X$  consists of  $P$  variables  $x_i (i = 1, \dots, p)$ . The parameter  $a_{ij} (i = 1, \dots, p; j = 1, \dots, K)$  represents the weight of the link connecting the input node  $i$  to node  $j$  in the hidden layer, in which  $K$  is the number of nodes in the hidden layer. The parameter  $W_j$  represents the weight of link connecting the hidden node  $j$  to the node in the output layer, and the variable  $d$  represents the weight of the bias. The bias term (a constant value, typically one) allows the neural network to return a nonzero value at the origin.  $a_{ij}, W_j$  and  $d$  are parameters needed to be estimated using a learning algorithm which will be discussed later.

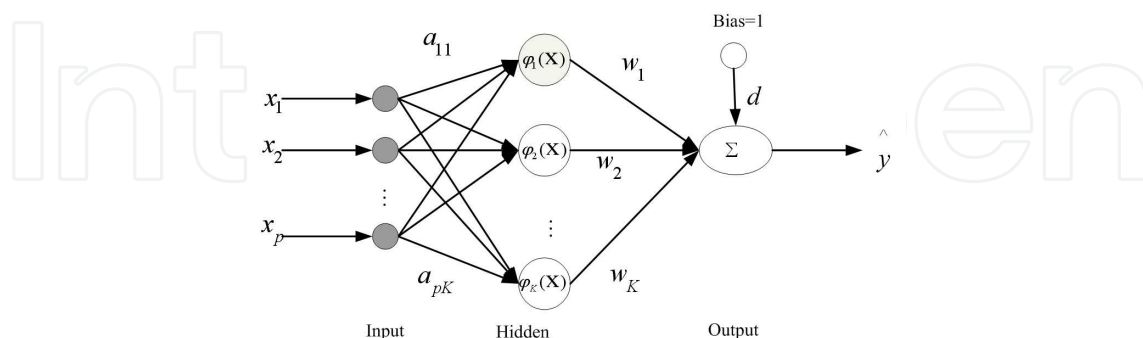
Let  $\theta = \{a_{ij}, W_j, d\}$  represent the group of parameters to be estimated. The model output  $\hat{y}$  is conceptually expressed as (Rumelhart et al., 1986):

$$\hat{y} = f(x, \theta) \quad (2-14)$$

In training an ANN model, a measure of the error  $e$  is often used as a model -quality index. The error is defined as the difference between the actual and predicted values, expressed as:

$$e = y - \hat{y} \quad (2-15)$$

A well-trained model should yield small prediction errors, which is often used to assess the validity of the trained model.



$x = [x_1, \dots, x_p]$  = Input vector containing  $P$  variables.

$a_{ij}$  = Weight of the link connecting the input node  $i$  to node  $j$  in the hidden layer.

$W_j$  = Weight of the link connecting the hidden node  $j$  to the node in the output layer.

$d$  = Weight of the bias.

$y$  = Model output.

Fig. 2.2 An illustrative example for feedforward three-layer ANN model

The ANN is suitable particularly for problems that are too complex to be modeled and solved by classical mathematics and traditional procedures, such as engineering design and image recognition. Typical ANN models include back-propagation (BP) neural network, radial basis function (RBF) neural network, Boltzmann neural network and dynamic neural network. One of the reasons for popularity of the neural network is the development of the error back-propagation training algorithm, which is based on a gradient descent optimization technique. The principle of BP network will be introduced briefly in the following section.

### 2.3.2 Principle of BP network

The error back-propagation neural network is called BP network for short. This algorithm makes training sample outputs and target outputs as a nonlinear optimization problem. By using gradient descent method, the weights can be obtained between nodes (Hagan & Menhaj, 1994). Actually, BP network reflects the mapping relationship between the input and output in the form of weights.

The structural model of a BP network is shown in Fig.2.3 which consists of an input layer, a hide layer and an output layer (Ripley, 1996). First the input layer receives characteristic parameter information, then the hide layer studies and processes input information and connects the input layer and the output layer by weights, last the output layer compares with target value continually and propagates the error back.

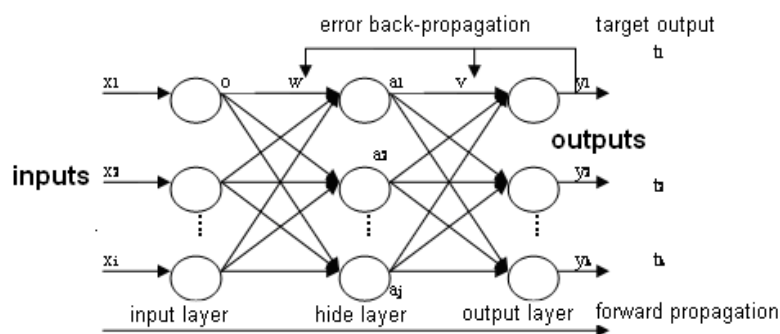


Fig. 2.3. The structure model of BP network

The weight from input layers to hide layers and the one from hide layers to output layers are corrected continually by forward propagation and back propagation. The inherent law of input samples can be found afterwards. In Fig.2.3,  $x$  is the input characteristic parameter;  $i$  is the number of input nodes;  $w$  is the weight from input layers to hide layers;  $a$  is the output of the hide layer;  $j$  is the number of hide layer nodes;  $v$  is the weight from hide layers to output layers;  $y$  is the output of output layers;  $k$  is the number of output layer nodes;  $t$  is the target value of the network.

Process of forward propagation can be described as follows: Input layer: Adopt the linear input function and equal any output  $o_i$  to its input  $x_i$ ; Hide layer: Any input  $net_j$  is the weighted sum of forward outputs  $o_j$ ,  $net_j = \sum w_{ji}o_j + \theta_i$ , here  $\theta_i$  is the threshold of hide layer nodes. The output is  $a(j) = f(net_j)$ ;  $f$  can be represented by the *sigmoid* function as  $f(net_j) = 1 / (1 + \exp(-net_j))$ ; Output layer: the weighted sum of hide layer outputs is the input of output layer. Adopting linear output function makes the  $k$ th output  $y_k$  be  $y_k = \sum_j v_{kj}a_j$ , where  $k$  is an integral number.

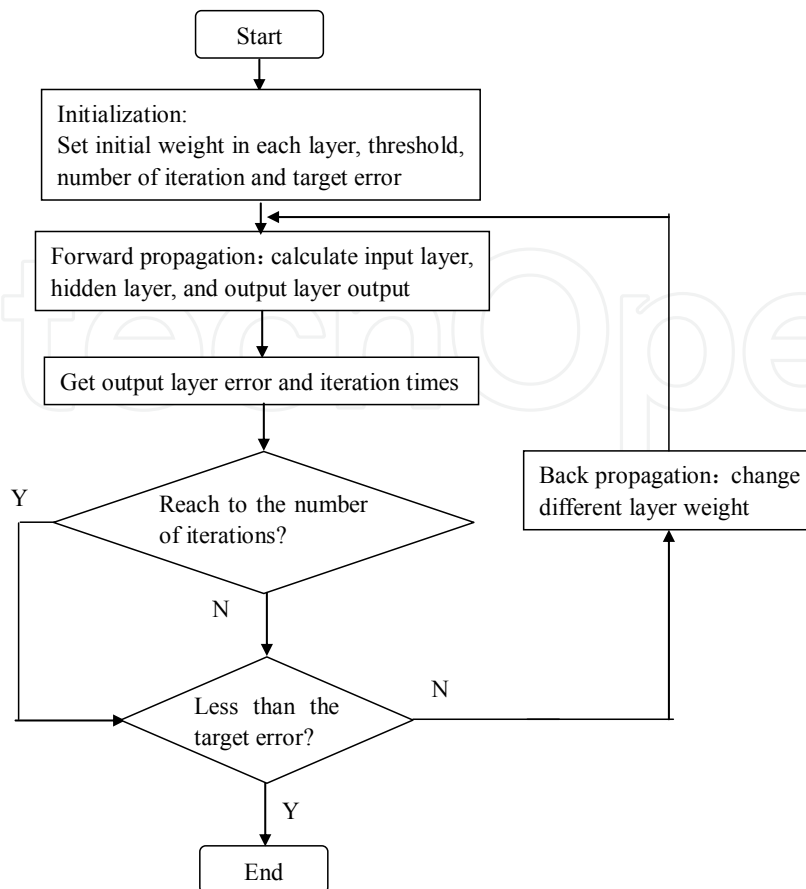


Fig. 2.4. BP network learning process

During processing of back propagation, the error function  $E_p$  is defined by  $E_p = \frac{1}{2} \sum_k (t_k - y_k)^2$ ; if the output error is not satisfied with the requirement, the network propagates errors back to modify the weight.

For weight correction, the learning algorithm of BP network adopts gradient descent method to adjust the weight value. Adjusted quantity is fixed as  $\Delta W_{kj} = -\eta \frac{\partial E_p}{\partial W_{kj}}$ . From this formula we can obtain the weight correction between hide layers and output layers as  $\Delta_{kj} = \eta \xi_k a_j$ . Here  $\eta$  is learning rate, and  $\xi_k = y_k(1 - y_k)(t_k - y_k)$ ; the weight correction between input layer and hide layer is  $\Delta w_{ji} = \eta \xi_j o_i$ , here  $\xi_j = a_j(1 - a_j) \sum_k \xi_k v_{kj}$ . The BP network learning process is shown in Fig.2.4.

### 3. Design of the virtual SLM

#### 3.1 Structure of the virtual SLM

The overall structure of the virtual SLM is decided to adopt PC plug-in virtual instrument mode, namely "A/D + PC + software" which is shown in Fig.3.1 (Pedro & Fernando, 2010). The microphone is the device to convert the measured source of sound signal to electrical

signal. The A/D card inserted in PC slot is used to convert the analog electrical signal into digital signal. The Personal computer is applied to carry out the signal analysis and processing. Here the PXI-4472 A/D card from National Instruments Company is chosen. LabVIEW platform is used to develop the software of the virtual SLM to read the converted A/D signal and complete the signal analysis, computation, storage and display (Cao & Luo, 2007).

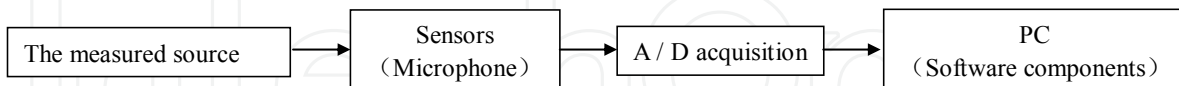


Fig. 3.1. Hardware structure of virtual SLM

### 3.2 Software structure

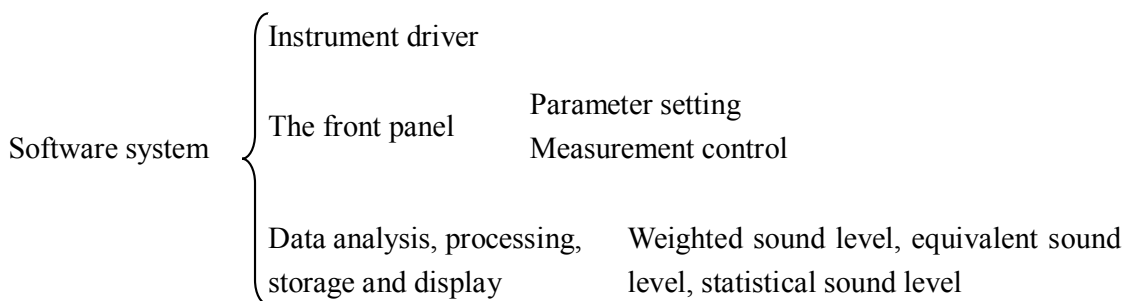


Fig. 3.2. Software structure of virtual SLM

As shown in Fig.3.2, the front panel is mainly responsible for the configuration of measured parameters, display of the measured results, etc. The function of data collection, analysis and processing are realized in the block diagram program.

### 3.3 Front panel control program

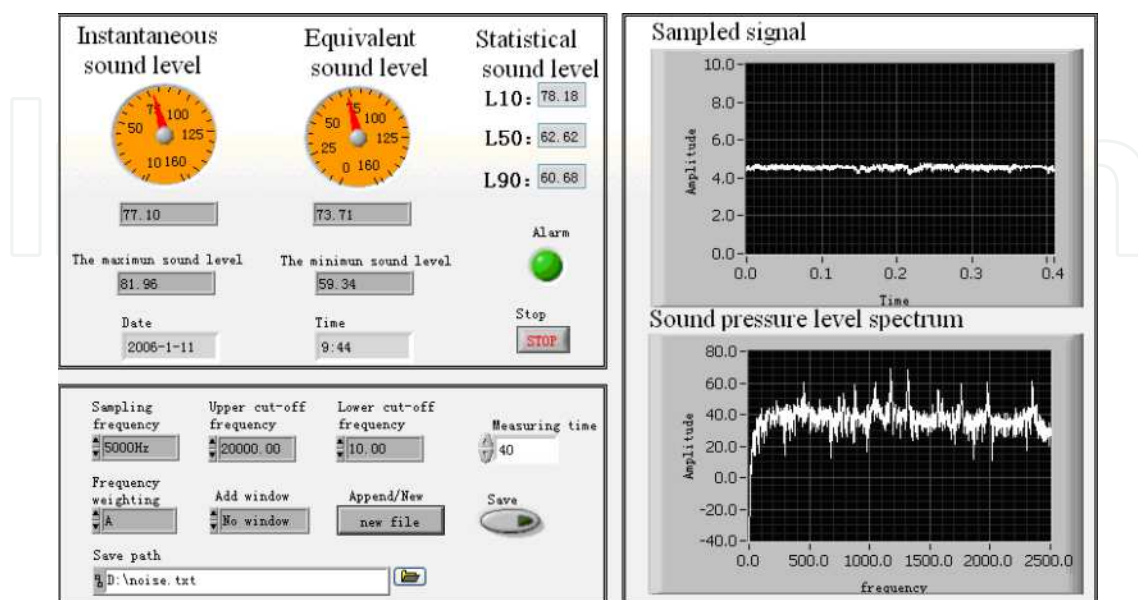


Fig. 3.3. The front panel of the virtual SLM

As shown in Fig.3.3, the front panel is mainly divided into three modules: result display module, parameter setting module and waveform display module. It is necessary to configure the measuring parameters that mainly include sampling frequency, add window type, filter fluctuation cut-off frequency, measuring time and frequency of weighted pattern (A, B and C), file path and preservation method. The measurement results mainly include the instantaneous sound level, equivalent continuous sound level, statistical sound level, the maximum- minimum sound level, alarm lamp, and the current date time, etc.

### 3.4 Procedure of signal processing of the virtual SLM

As shown in Fig.3.4, LabVIEW first reads the signal from A/D channel, and then processes adding window, filtering and other preprocessing to suppress the interference composition, next calculates unilateral power spectrum, converts the signal to frequency domain. After effective value transform, calculation of each frequency sound pressure, frequency weighting from instantaneous sound level at each sampling period are fulfilled. Finally based on instantaneous sound level, maximum/minimum sound level, statistical sound level and continuous equivalent sound level can be calculated (Luo et al., 2008)

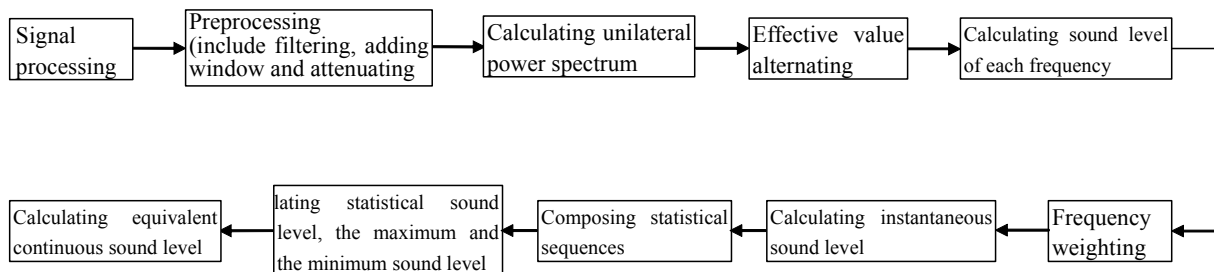


Fig. 3.4. Procedure of signal processing of the virtual SLM

### 3.5 Preprocessing

Signal often contains undesired noise, especially electrical noise signal. So filtering is needed for preprocessing. The bandpass filter is applied since upper and lower cutoff frequency can be dynamically adjusted according to requirement. In order to reduce the spectrum leakage due to signal truncation, adding windows processing is applied. The window function can be Hanning windows, Hamming windows, or Blackman windows, etc. The program is shown in Fig.3.5.

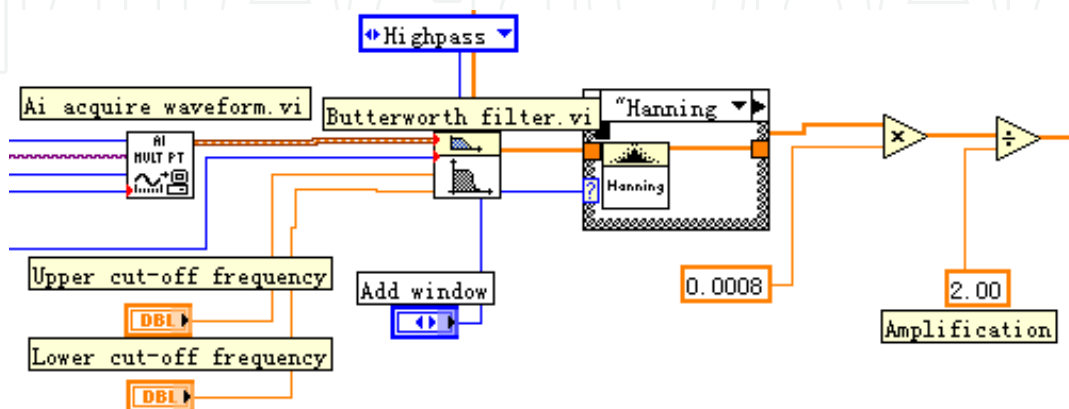


Fig. 3.5. Preprocessing program

### 3.6 Frequency weighting

#### 1. Least squares

In scientific experiment data processing, it is a common task to seek out the function relationship between independent variable  $x$  and dependent variable  $y$  as  $y = f(x; a_0, \dots, a_n) (n < m)$ , here  $a_i$  is undetermined parameters from a set of experimental data as  $(x_i, y_i), i = 0, 1, \dots, m$ . In general, observation data have errors and the undetermined parameter number is less than that from experiment. This kind of problem is different from interpolation and function  $y = s(x) = s(x; a_0, \dots, a_n)$  is not required to pass through the data points  $(x_i, y_i)$ , and only requires that the sum of squares  $\sum_{i=0}^m \delta_i^2$  of  $\delta_i = s(x_i) - y_i (i = 0, 1, \dots, m)$

is smallest at the given data points. This is the so-called least-square approximation. The least-square fitting curve  $y = s(x)$  can be obtained thereby. This approach is called curve fitting least-square method. Frequency weights at each frequency are obtained by using the least-square method in the frequency weighting module.

#### 2. Frequency weighting

Weighted network is an important part of SLM which directly affects the accuracy of various sound levels. As shown in Fig.3.6, the approach is to fit the frequency weighted value of A, B, C provided by IEC651 "sound level meter" into curves using least-squares polynomial fitting method in MATLAB. According to the curves, the required frequency weighting correction values are calculated and stored in array  $x$ , the unilateral power spectrum sequence of the input signal are calculated and stored in array  $L$ . Then the sum of  $L$  and  $x$  is the corresponding frequency weighting result of the signal. According to the frequency weighted signal, sound pressure level is calculated for one sampling period. That is the value of the instantaneous sound level.

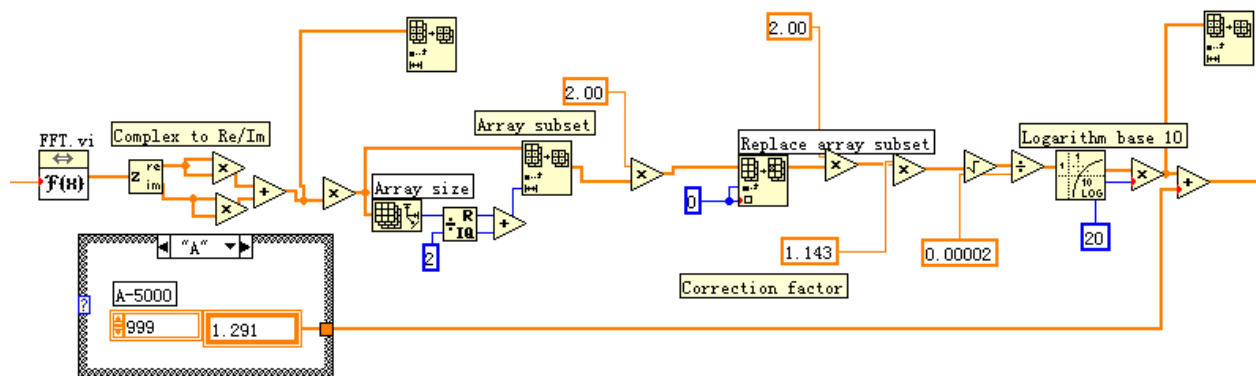


Fig. 3.6. Frequency weighting

### 3.7 Statistical analysis

As shown in Fig.3.7, in order to perform statistical analysis of sound level, the instantaneous sound level is input to a statistical array in a loop and then sort operating is carried out. It is easy to get the statistical sound levels  $L_{10}, L_{50}, L_{90}$  the largest and smallest sound level  $L_{\max}, L_{\min}$ . In addition, the time of statistical analysis is changed by adjusting the length of the statistical array.

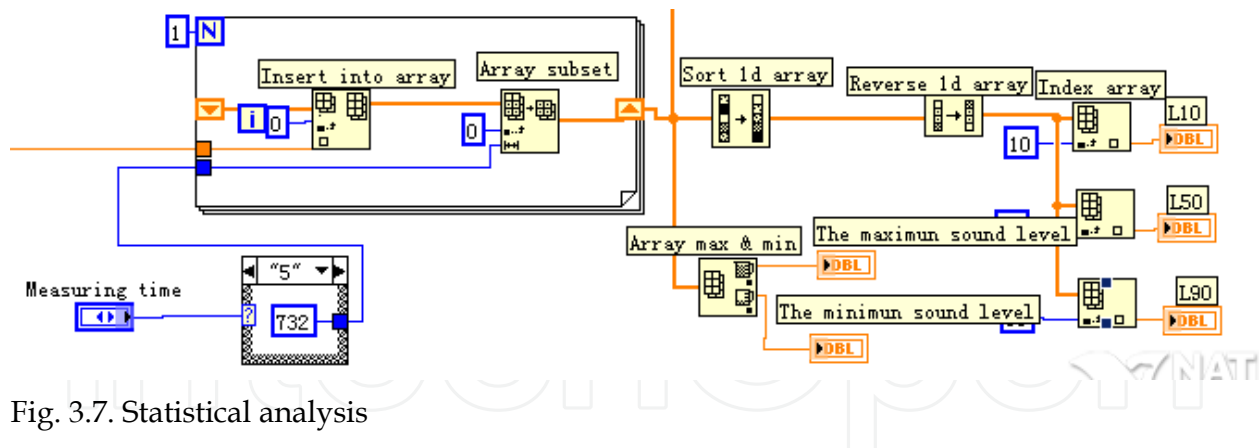


Fig. 3.7. Statistical analysis

### 3.8 Equivalent continuous sound level

Calculation of equivalent continuous sound level is carried out according to Equation (2-3). The program is implemented as shown in Fig.3.8. The control of the equivalent time namely measurement time is achieved by varying the length of statistical sequence.

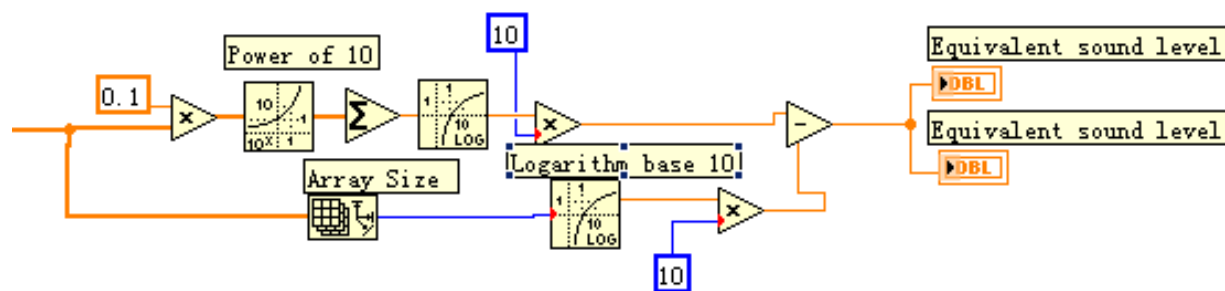


Fig. 3.8. Calculation of equivalent continuous sound level

### 3.9 Frequency spectrum analysis, preservation and alarm

Spectrum analysis, preservation and alarm function etc. are realized by calling the appropriate controls in LabVIEW.

### 3.10 Calibration of the system magnification

TES-1356 sound pressure calibrator from Taishi Company, Taiwan is selected to calibrate the virtual SLM system. The output frequency of TES-1356 is 1000HZ ( $\pm 4\%$ ). The two standard output sound pressure levels are 94dB and 114dB with accuracy within  $\pm 0.5$ dB respectively. Calibration experiments have been carried out. The measured sound pressure levels are compared with the standard pressure levels to get the errors when the magnification factor is varied from 1.0 to 2.2. The experimental data are given in Table 3-1.

In the table,  $\Delta x1 = \frac{L_x - 94}{94} \times 100\%$ ,  $\Delta x2 = \frac{L_x - 114}{114} \times 100\%$ .  $L_x$  is the actual sound level and

$\Delta x1$ 、 $\Delta x2$  respectively represent the error rate under 94dB and 114dB standard value. Considering the values of  $\Delta x1$  and  $\Delta x2$ , the system magnification factor is determined to be 1.9. Since the calibrator generates a pure tone at 1000Hz, the calibration at this frequency means calibrating the entire system at all frequencies excluding the frequency weighting model. Moreover the applied A-weighted correction values fall into the tolerance range of 0-type sound level meter specified by the IEC651 standard "sound level meter".

Multiple Sound pressure	1.0	1.2	1.4	1.6	1.7	1.74	1.76	1.78	1.80	1.90	2.0	2.1	2.2
94dB	99.48	97.88	96.52	95.38	94.84	94.63	94.49	94.42	94.32	93.89	93.41	92.99	92.58
$\Delta x_1$	5.83	4.13	2.68	1.47	0.89	0.67	0.52	0.45	0.34	-0.12	-0.63	1.07	-1.51
114dB	119.92	118.33	116.99	115.83	115.32	115.10	115.02	114.88	114.80	114.32	113.86	113.48	113.06
$\Delta x_2$	5.1	3.8	2.62	1.61	1.16	0.96	0.89	0.77	0.7	0.28	-0.12	-0.46	-0.82

Table 3-1. The experimental data of system calibration

### 3.11 Comparative experiment

Time(s)	5	10	15	20	25	30	35	40	45	50
Sound level A										
Sound level (dB)	59.3	59.7	59.4	59.0	59.6	59.7	59.8	59.0	59.2	59.4
Time(s)	55	60	65	70	75	80	85	90	95	100
Sound level A										
Sound level (dB)	59.7	59.1	59.6	59.3	59.3	59.6	60.0	59.4	59.3	59.6

Table 3-2. The instantaneous sound level A ( $L_A$ ) Measured by TES–1357 per 5 seconds

Comparative experiments between the virtual SLM and a commercial SLM TES-1357 with an accuracy of  $\pm 1.5$ dB from Taishi Company of Taiwan have been carried out. In the relatively quiet and closed environment, generate a stable sound field with PXI-1002 from NI is generated, and then the microphone of TES-1357 and the microphone of this system are placed into the same location of the stable sound field. Experiment is performed and data are given in Table 3-2 and Table 3-3.

Time (s)	5	10	15	20	30	40	50	100	150
The average value of sound level A during N seconds (dB)	59.31	59.50	59.04	59.90	59.25	59.59	59.50	59.52	59.55

Table 3-3. The average value of instantaneous sound level A ( $L_A$ ) measured by the virtual SLM during N seconds

As shown in Table 3-2, the average value ( $\bar{L}_A$ ) of 20 instantaneous sound level A is 59.45dB. The average value of instantaneous sound level A is 59.52dB within 100 seconds and the average value is 59.55dB within 150s as shown in Table 3-3. Compared with the average value 59.45dB measured by TES-1357 within 100s, the errors of the virtual SLM are +0.07dB, +0.1dB respectively. TES-1357 is a precise sound level meter with an accuracy of  $\pm 1.5$  dB. The comparative experiment verifies that the accuracy of the virtual SLM is acceptable. The maximum error between A-weighted correction value in this system and the value specified by IEC651 is 0.3113dB which implies that the tolerance requirement of type-0 SLM is met. The sound level meter is calibrated by a standard sound level calibrator. The errors of the virtual SLM compared with the calibrator at 94dB, 114dB are 0.11dB, 0.32dB, respectively. It indicates the measurement error of the developed virtual SLM is under  $\pm 0.5$ dB and thus the precision achieves the requirements of type-1 SLM.

## 4. An online fan fault diagnosis system based on wavelet and neural network under LabVIEW platform

### 4.1 Implementation of wavelet de-noising on LabVIEW

#### 4.1.1 Wavelet decomposition for signal with noise in each layer

As shown in Fig.4.1, original signal "signal" is convolved with "wfilters" which denote low-pass and high-pass filter coefficients. Then the result is down-sampled to get approximate coefficients  $ca\_n$  and detailed coefficients  $cd\_n$  respectively. At the same time, the length (size) of the approximate coefficients in each layer is returned. "level" denotes the number of decomposition layer. "wname" denotes the used wavelet name, and "wfilters" denotes the corresponding filter coefficients used by the wavelet which are computed by "wfilters" function in MATLAB. The program is shown in Fig.4.1.

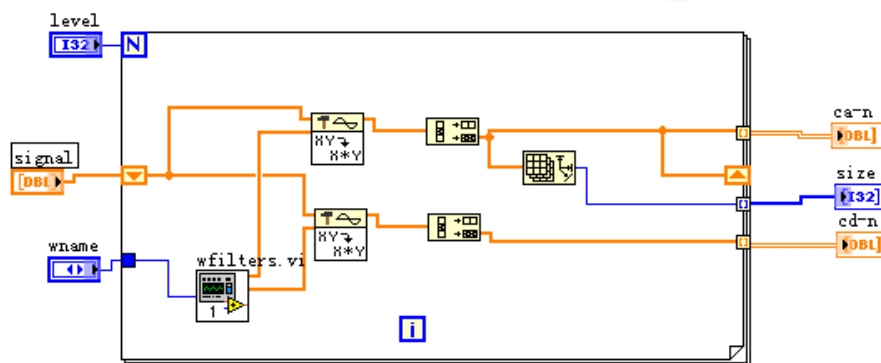


Fig. 4.1. Block diagram of wavelet decomposition

#### 4.1.2 Thresholding for high frequency coefficients

##### 1. Determination of threshold

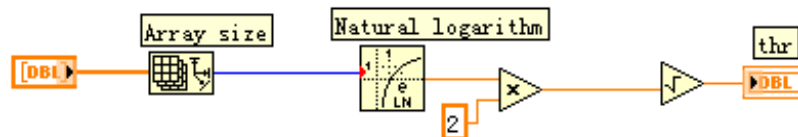


Fig. 4.2. Determination of threshold

Determination of threshold is a key step in signal de-noising based on wavelet since threshold selection has direct impact on the effect of de-noising. The determination of threshold can be realized by *Thselect* command in MATLAB. As shown in Fig.4.2, 'sqrtwolog' in *Thselect* command is adopted, so  $thr = \sqrt{2 \ln N}$ , where  $N$  denotes the length of high frequency coefficient. This program is shown in Fig.4.2.

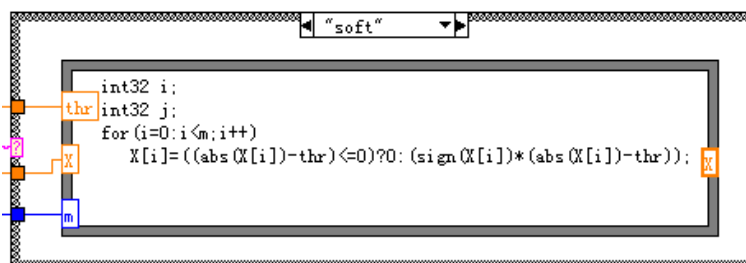


Fig. 4.3. Threshold processing

## 2. Thresholding

Modes of thresholding action are divided into hard thresholding and soft thresholding. Soft thresholding can be expressed as a mathematical formula:

$$X_{thr} = \begin{cases} \text{sign}(x)(|x| - thr) & |x| > thr \\ 0 & |x| < thr \end{cases} \quad (4-1)$$

Hard thresholding can be expressed as:

$$X_{thr} = \begin{cases} x & |x| > thr \\ 0 & |x| < thr \end{cases} \quad (4-2)$$

In Equation(4-1) and (4-2),  $x$  denotes the element of high frequency coefficient,  $thr$  denotes the selected threshold, and  $X_{thr}$  denotes a sequence after thresholding. Here threshold processing of the high frequency coefficients is achieved by utilizing Formula Node control as shown in Fig.4.3.

### 4.1.3 Reconstruction of low frequency coefficients and high frequency coefficients processed by thresholding

As shown in Fig.4.4, the process of reconstruction is as follows (Cao et al., 2009):

1. The N-layer approximate coefficient  $ca_n$  is up-sampled, then the result is convolved with the low-pass filter coefficients of the applied wavelet to get  $ca_{conv}$ . While the n-layer detail coefficient  $cd_n_{thr}$  is processed in the same way,  $cd_{conv}$  is obtained and high-pass filter coefficients of the same wavelet are used when carrying out convolution.
2.  $ca_{ret}$  is obtained by extracting ret elements from the sequence  $ca_{conv}$  starting at the  $k$ th element. The calculation of ret is expressed as,  $ret_w = \text{the length of } ca_n * 2 - \text{the length of filter} + 1$ . If  $ret_w$  is odd, then  $ret = ret_w + 1$ ; If  $ret_w$  is even, then  $ret = ret_w$ .  $k = (\text{the length of } ca_n - \text{the length of } ret) / 2$ .  $cd_{ret}$  can be obtained while the thresholded n-layer detail coefficient  $cd_n_{thr}$  is processed in the same way.
3. The de-noised signal  $ca_{n-1}$  is obtained from adding  $ca_{ret}$  with  $cd_{ret}$ .
4. Then the (n-1)th wavelet reconstruction is made by use of  $ca_{n-1}$  and  $cd_{n-1}_{thr}$ . Repeat until the first layer.

The program for one layer wavelet de-noise of a signal is shown in Fig.4.5, where  $wname$  is the name of the used wavelet, and  $mode_{opera}$  denotes the mode of threshold action *hard* or *soft*.

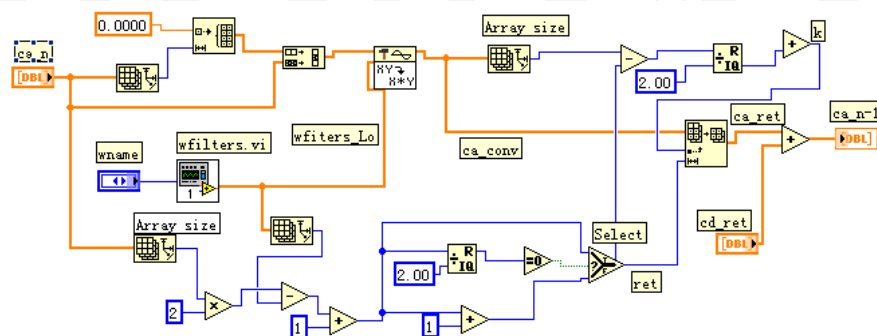


Fig. 4.4. Reconstruction of single-layer wavelet

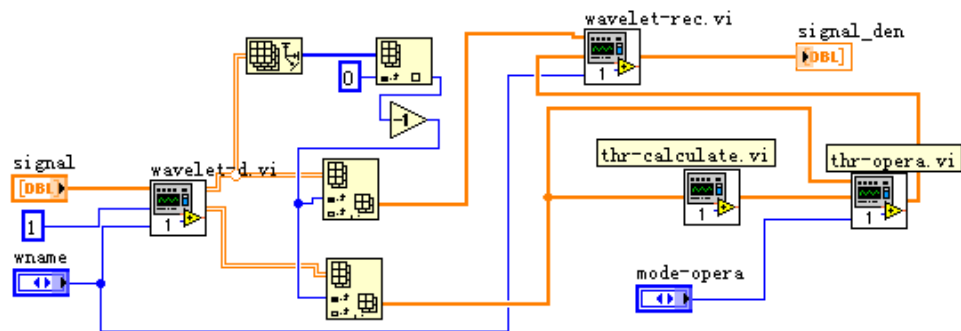


Fig. 4.5. Signal single-layer de-noising

#### 4.2 Feature extraction based on wavelet

Since it is different that system faults suppress or enhance the noise signal energy with distinct frequency, the proportional relationship of the signal energy with different frequency contains abundant fault information. Proportion of certain frequency band energy represents certain fault feature. Therefore it is an important method based on wavelet feature extraction by using the diagnosis method of “energy ---fault”. The realization steps are as follows (Cao et al., 2009):

1. Wavelet decomposes the collected signal to obtain each layer's details and approximate coefficient, and thresholdly process high frequency coefficients.
2. Reconstruct the low-frequency coefficients and high frequency coefficients after thresholdly processing, and obtain corresponding frequency signal.
3. Calculate frequency band energy corresponding to the square of frequency signal.
4. Create feature vector. Creating feature vector is based on relevant frequency band energy for the elements.

Whether you find an accurate vector that represents fault plays a key role for successful diagnosis or not. It is very important to choose the feature vector in fault diagnosis.

#### 4.3 Fault diagnosis based on neural network

Fault diagnosis based on neural network includes the following steps (Cao et al., 2009):

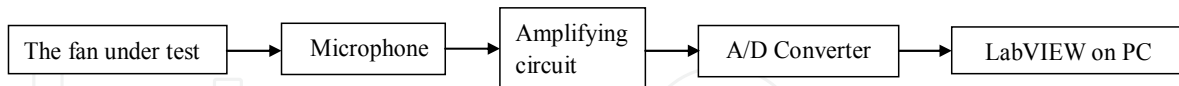
1. Data acquisition and feature extraction for feature vector.
2. Network structure design. According to dimension number of the input feature vector and equipment fault status, the node number of the input and output layers of neural network can be determined. The node number of the hidden layer is selected on experience.
3. Network training. The extracted feature vectors are input vectors. Collect a certain amount of input data as training samples to train the network. When the network output error is less than the goal error, exit and save the network parameters.
4. Fault diagnosis. Input the sample data into the neural network and get the diagnosis result for the fault status.

#### 4.4 Design of the online fan fault diagnosis system

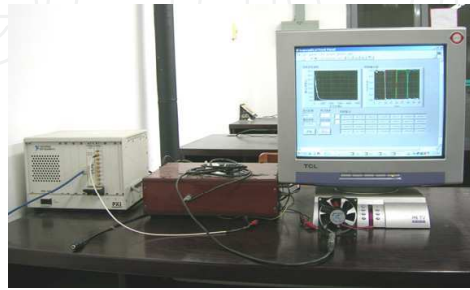
##### 4.4.1 Structure of the hardware system

The structure of the hardware system of an online fan fault diagnosis system is shown in Fig.4.6 which consists of the diagnosed object, microphone, amplifying circuit, A/D converter card, and a personal computer with LabVIEW platform. The microphone converts

the signal produced by fan into voltage signal. The amplifying circuit conditions the signal to a required scope. The A/D converter card PXI-4472 from NI Company acquires the signal and converts it to digital signal. Then the digital signal is accessed to LabVIEW by the software of the online wavelet neural network fan fault diagnosis system.



(a) Structure of the hardware system



(b) Photo of the hardware system

Fig. 4.6. Structure of the hardware system

#### 4.4.2 Design of the software system

As shown in Fig.4.7, the software system comprises three parts of training sample, network training and on-line diagnosis. The function of each part is described as follows.

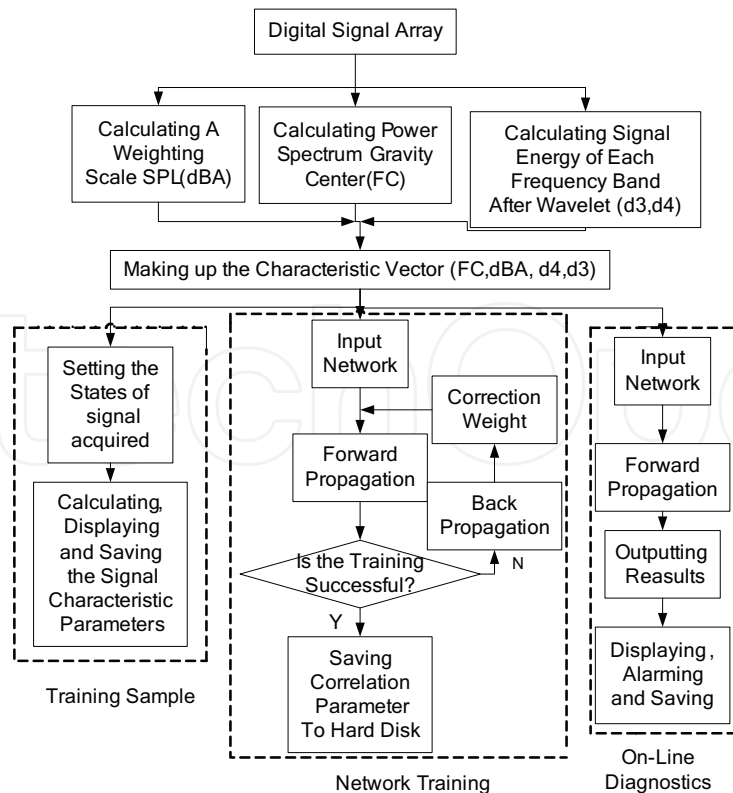


Fig. 4.7. Structure of the software system

Training sample: relying on the target under test sets frequency of sampling, number of samples, sample size, state of sampling signal such as normal state, paper choking, eccentric blade, blade breaks, and so on, acquire a certain number of samples of signal in different states. Then, calculate the feature vector of each state and save the vector to a specified location.

The function of network training: set the node number of input layer, hide layer and output layer; initialize the weights and threshold values of each layer; train network and save the correlation parameter for calling.

On-Line diagnostics: acquire the noise signal of fan; calculate the feature vector; input the trained network; output and save the fault probability and alarm message.

#### 4.4.3 Extracting the feature vector

How to choose characteristic parameters directly affects the performance of diagnosis system. In the proposed system, the feature vector consists of A-weighted sound level, power spectrum gravity centre and signal energy of each frequency band after wavelet decomposition.

The power spectrum gravity center (FC) is calculated by:

$$FC = \frac{\sum_{i=1}^N f_i p_i}{\sum_{i=1}^N p_i} \quad (4-3)$$

where,  $f_i$  is the frequency,  $p_i$  is the magnitude and  $i$  is the order of the power spectrum line. If fault occurs, the magnitudes of some frequency will change and affect the position of power spectrum gravity center, the energy distribution of different frequency band after wavelet decomposition and the measuring results of A-weighted sound level.

#### 4.4.4 Experiments

Four fans RDM8025S made by RUILIAN SCIENC company of China, are used for the fault diagnosis experiment. One fan is normal, the other three are paper choking, eccentric blade, and blade breaks respectively.

##### 1. Network structure design

Suppose FC stands for the frequency power spectrum gravity center. A-weighted sound level is dbA.  $d_3$  and  $d_4$  respectively stand for the energy distribution of the third and fourth frequency band after wavelet decomposition. The feature vector  $x = (FC, dbA, d_4, d_3)$  is input of the network. The fault modes such as normal  $y_1$ , paper choking  $y_2$ , eccentric blade  $y_3$  and blade breaks  $y_4$  are composed of the output vector  $y = (y_1, y_2, y_3, y_4)$ . For example,  $y = (0, 1, 0, 0)$  shows that the fan fault is paper choking.

The node number of input layer equals four which is the dimension of  $x$ . Similarly, the node number of output layer equals the dimension of  $y$ . The node number of hide layer is empirically two. Linear action function is chosen at input and output layer. The action function of hide layer is the *sigmoid* function.

##### 2. Signal acquisition

Set the sampling frequency as 5000 Hz and the number of samples as 2048.  $db_2$  is used by wavelet and the decomposition level is four. Under each one of four states, we acquire ten sets data in which two sets are selected to calculate the feature vector. The results are shown in Table4-1.

Number of Samples	x1	x2	x3	x4	Mode
1	200.170	78.350	46.306	27.273	Normal
2	190.829	77.913	44.669	23.890	Normal
3	300.180	83.114	61.277	32.537	Paper choking
4	295.919	82.746	59.160	33.841	Paper choking
5	132.724	80.684	65.717	28.857	Eccentric blade
6	134.868	81.450	83.176	38.774	Eccentric blade
7	113.926	74.022	31.793	18.459	Blade breaks
8	122.163	75.550	36.515	19.621	Blade breaks

Table 4-1. Characteristic value of training sample acquired and the corresponding fault modes

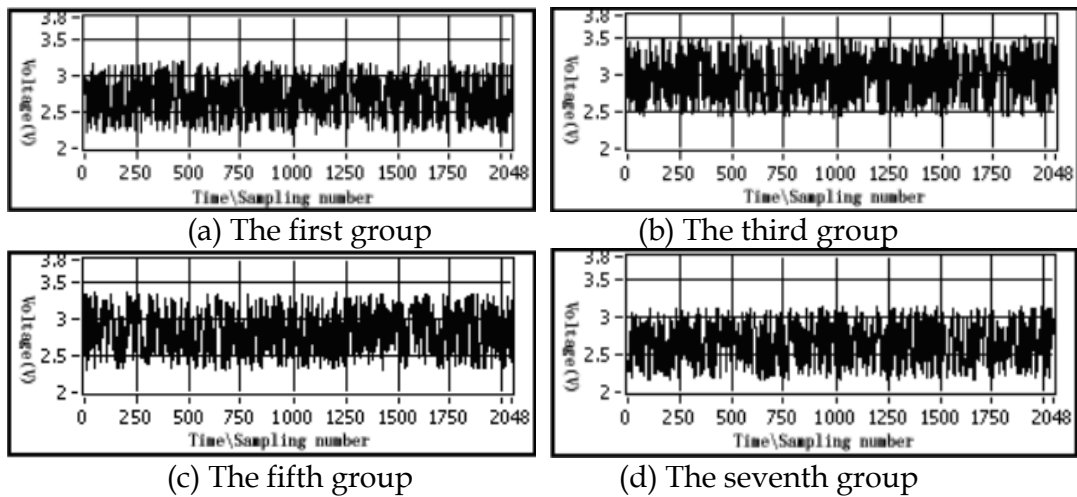


Fig. 4.8. Time-domain waveforms of signal sample

For the first, third, fifth, and seventh set of signal samples time domain waveforms are respectively listed in Fig.4.8. The front panel of acquisition process is shown in Fig.4.9.

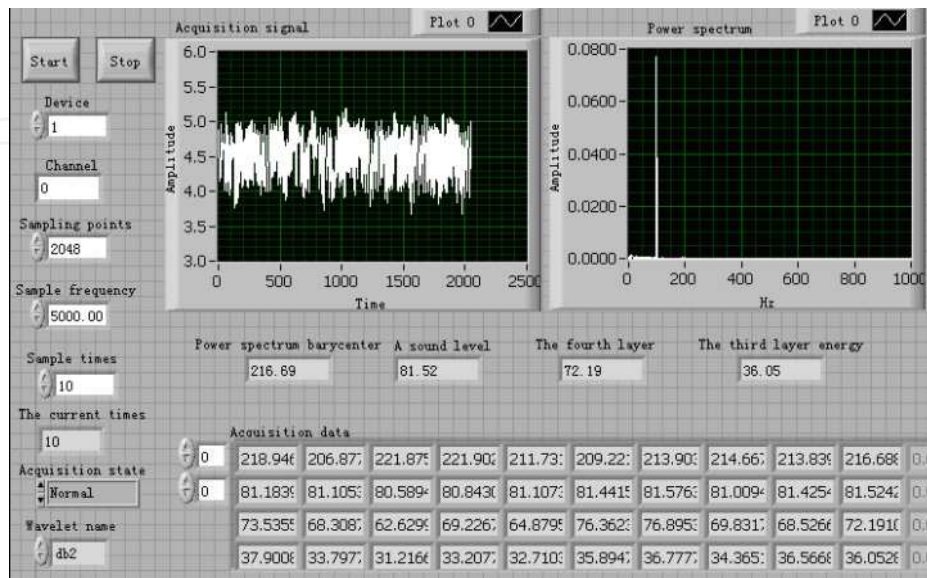


Fig. 4.9. The front panel of signal acquisition module

3. Network training

To keep a stable learning rate and avoid network oscillation, the learning rate, weight and the error of target should be selected suitably while executing the network training. If the learning rate is too fast, there will be a constant oscillation in the network that makes it difficult to achieve the target value. If the error of target is too small, the requirement of specified iteration number can not be achieved. The initial weight and threshold value are set as the random number between 0 and 1. In experiment, the error of target and the maximal iteration number are set as 0.05 and 5000 respectively.

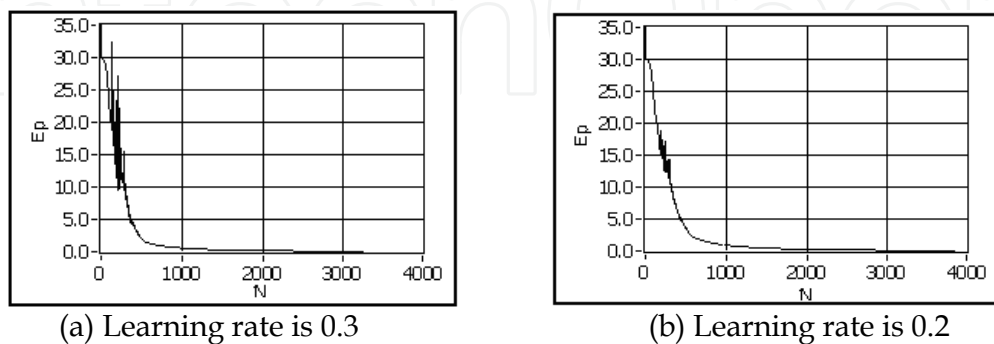


Fig. 4.10. Relationship between output error  $E_p$  and iteration number  $N$

After the network is trained, the relationship between actual output error  $E_p$  and iteration number  $N$  is shown in Fig.4.10. In the figure (a), the learning rate is 0.35. A large oscillation occurs during training. In the figure (b), the learning rate is 0.2. However, the oscillation during the training is small. When the output error is decreased from 31.2 to 0.049997 and the required value is reached, the iteration number is 3677. The fault mode of training sample ( $t_1, t_2, t_3, t_4$ ) and the actual output of network ( $y_1, y_2, y_3, y_4$ ) is listed in Table4-2. It can be seen from Table4-2 that the fault mode of acquired samples has already been recognized accurately by the network. Last, the related parameters of this network are stored in the specified location. The front panel of the training process is shown in Fig.4.11.

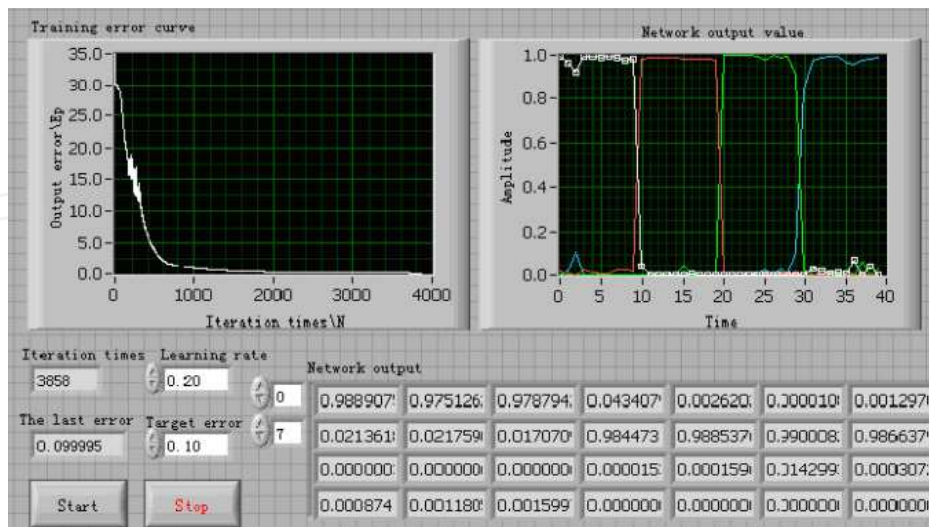


Fig. 4.11. The front panel of network training module

4. On-line diagnosis

The well trained network is used to diagnose the fan under test to acquire the noise signal produced by fan working at each mode. Using the sampling value, the corresponding

feature vector is calculated for input to the well trained network in order to perform on-line diagnosis. Table 4-3 lists the characteristic parameters and the corresponding network outputs.

Number of samples	Fault modes				Outputs of network			
	t1	t2	t3	t4	y1	y2	y3	y4
1	1	0	0	0	0.9695	0.0104	0.0002	0.0005
2	1	0	0	0	0.9769	0.0087	0.0001	0.0009
3	0	1	0	0	0.0567	0.9804	0.0007	0.0000
4	0	1	0	0	0.0441	0.9754	0.0021	0.0000
5	0	0	1	0	0.0003	0.0000	0.9921	0.0054
6	0	0	1	0	0.0005	0.0000	0.9434	0.0236
7	0	0	0	1	0.0268	0.0000	0.0325	0.9194
8	0	0	0	1	0.0299	0.0000	0.0146	0.9858

Table 4-2. Fault modes of training samples and outputs of network

Testing sample	Characteristic parameters				Outputs of network			
	x1	x2	x3	x4	y1	y2	y3	y4
1 (Normal)	221.104	79.039	46.127	24.898	0.976	0.047	0.001	0.000
2 (Paper hoking)	273.696	81.797	54.367	31.075	0.016	0.980	0.005	0.000
3 (eccentric lade)	135.684	78.717	60.857	26.812	0.003	0.060	0.994	0.010
4 (balde breaks)	110.927	74.364	31.303	17.032	0.002	0.000	0.044	0.997

Table 4-3. Characteristic parameters of testing sample and outputs of network

Compared to Table 4-3 with Table 4-2, we can find that although the feature vectors of fan under test are different with the training samples, the proposed system can diagnose the fault accurately. The front panel of online diagnosis module is shown in Fig.4.12.

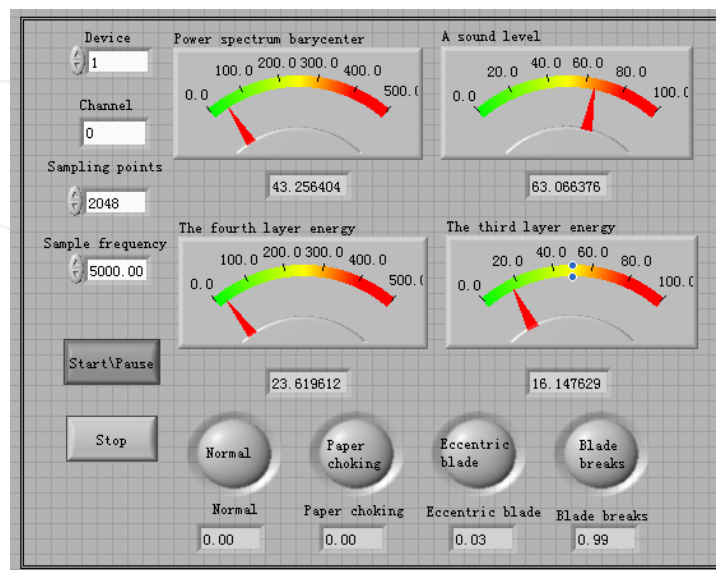


Fig. 4.12. The front panel of no-line diagnosis module

## 5. Conclusion

The proposed virtual SLM is calibrated by using TES-1356 sound level calibrator. Its accuracy is verified by the comparative experiment with TES-1357. The results indicate the measurement error is within 0.5 dB and the precision meets the requirements of the type I sound level meter.

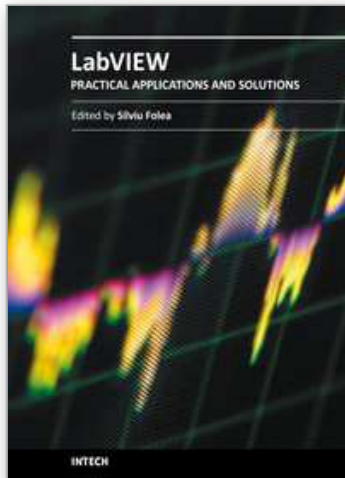
In the proposed intelligent fault diagnosis system, the noise produced by fan is diagnosis signal, non-connect measurement is adopted and using the wavelet neural network performs the non-linear mapping from feature space to defective space. Modular programming is adopted in this system, so it is easier to extend and change the characteristic parameters of fault and structure parameters of the network. Utilizing the learning, memory and reckoning abilities diagnoses the fault adaptively. The designed system has the better capacity of learning, deducing and fault tolerant. The diagnosis results are reliable and accurate.

## 6. References

- Adeli, H. & Jiang, X.J. (2009). *Intelligent Infrastructure: Neural Networks, Wavelets, and Chaos Theory for Intelligent Transportation Systems and Smart Structures*, CRC Press, ISBN 978-1-4200-8536-5, Boca Raton, FL
- Burrus, C.S. (2005). *Introduction to Wavelets and Wavelet Transforms*. China Machine Press, ISBN 7-111-15911-X, Beijing
- Cao, G.Z. & Ruan, S.C.(2002).Design of New Instrument Based on DSP for Measuring Car's Noise Combined with Rotating Speed. *Instrument Technique and Sensor(in Chinese)*, No.08, pp. 11-13, ISSN 1002-1841
- Cao, G.Z.; Wu, W. & Ruan, S.C. (2004). A New Method for Measuring the Rotary Speed of a Car's Engine Based on the Spacing Measurement of Its Noise and Its Implementation. *Journal of Xi'an Shiyou University( Natural Science Edition, in Chinese) ,Vol.19, No.05, pp. 81-86, ISSN 1001-5361*
- Cao, G.Z. & Luo, C.G. (2007). Design of Virtual Sound Level Meter in LabVIEW. *Instrument Technique and Sensor (in Chinese)*, No.06, pp. 16-18, ISSN 1002-1841
- Cao, G.Z.; Lei X.Y. & Luo C.G. (2009). Research of a Fan Fault Diagnosis System Based on Wavelet and Neural Network. *2009 3rd International Conference on Power Electronics Systems and Applications*, Digital Reference: K210509062, ISBN 978-1-4244-3845-7, Hongkong
- Donald, E. & Hall (1987). *Basic Acoustics*, Harper & Row, Publishers Inc. ISBN 0-06-042611-X, New York
- Hagan, M. T. & Menhaj, M.B. (1994). Training FeedForward Networks with the Marquardt Algorithm. *IEEE Trans on Neural Networks*, Vol.05, No.06, pp. 989-993, ISSN 1045-9227
- Kinsler, L.E.; Frey, A.R.; Coppens, A.B. & Sanders, J.V. (2000). *Fundamentals of Acoustics*. Wiley, John & Sons Inc. Pub., ISBN 0-471-84789-5, New York
- Luo, C.G.; Cao, G.Z. & Pan J.F. (2008). Design of a Fan Fault Diagnosis System Based on Wavelet and Neural Network. *Applied Acoustics(in Chinese)*, Vol.27, No.3, pp. 181-187, ISSN 1000-310X

- Mallat, S.G. (1989). A Theory for Multiresolution Signal Decomposition: the Wavelet Representation. *IEEE Pattern Analysis and Machine*, Vol.11, No.07, pp. 674-693, ISSN 0162-8828
- Mallat, S.G. & Hwang, W.L. (1992). Singularity Detection and Processing with Wavelet. *IEEE Trans on Inform Theory*, Vol. 38, No.02, pp. 617-643, ISSN 0018-9448
- Pedro, P.C. & Fernando, D. (2010). *Intelligent Control Systems with LabVIEW*, Springer, ISBN 978-1-84882-683-0, London
- Rumelhart, D.E.; Hinton, G.E. & Williams, R.J. (1986). Learning Representations by Back-propagating Errors. *Nature*, Vol.03, No.23, pp. 533-536, ISSN: 0028-0836
- Ripley, B.D. (1996). *Pattern Recognition and Neural Networks*, Cambridge University Press, ISBN0-521-46086-7, Cambridge
- Ruan, Z.K. & Cao, G.Z. (2006). An Acoustic Signal Data Acquisition System Based on DSP. *Electric Instrumentation Customer(in Chinese)*, Vol.13, No.05, pp. 44-46, ISSN 1671-1041

IntechOpen



## **Practical Applications and Solutions Using LabVIEW™ Software**

Edited by Dr. Silviu Folea

ISBN 978-953-307-650-8

Hard cover, 472 pages

**Publisher** InTech

**Published online** 01, August, 2011

**Published in print edition** August, 2011

The book consists of 21 chapters which present interesting applications implemented using the LabVIEW environment, belonging to several distinct fields such as engineering, fault diagnosis, medicine, remote access laboratory, internet communications, chemistry, physics, etc. The virtual instruments designed and implemented in LabVIEW provide the advantages of being more intuitive, of reducing the implementation time and of being portable. The audience for this book includes PhD students, researchers, engineers and professionals who are interested in finding out new tools developed using LabVIEW. Some chapters present interesting ideas and very detailed solutions which offer the immediate possibility of making fast innovations and of generating better products for the market. The effort made by all the scientists who contributed to editing this book was significant and as a result new and viable applications were presented.

### **How to reference**

In order to correctly reference this scholarly work, feel free to copy and paste the following:

Guangzhong Cao (2011). Acoustical Measurement and Fan Fault Diagnosis System Based on LabVIEW, Practical Applications and Solutions Using LabVIEW™ Software, Dr. Silviu Folea (Ed.), ISBN: 978-953-307-650-8, InTech, Available from: <http://www.intechopen.com/books/practical-applications-and-solutions-using-labview-software/acoustical-measurement-and-fan-fault-diagnosis-system-based-on-labview>

**INTECH**  
open science | open minds

### **InTech Europe**

University Campus STeP Ri  
Slavka Krautzeka 83/A  
51000 Rijeka, Croatia  
Phone: +385 (51) 770 447  
Fax: +385 (51) 686 166  
[www.intechopen.com](http://www.intechopen.com)

### **InTech China**

Unit 405, Office Block, Hotel Equatorial Shanghai  
No.65, Yan An Road (West), Shanghai, 200040, China  
中国上海市延安西路65号上海国际贵都大饭店办公楼405单元  
Phone: +86-21-62489820  
Fax: +86-21-62489821

© 2011 The Author(s). Licensee IntechOpen. This chapter is distributed under the terms of the [Creative Commons Attribution-NonCommercial-ShareAlike-3.0 License](#), which permits use, distribution and reproduction for non-commercial purposes, provided the original is properly cited and derivative works building on this content are distributed under the same license.

IntechOpen

IntechOpen